Journal of Alloys and Compounds 549 (2013) 100–104

Contents lists available at SciVerse ScienceDirect

Journal of Alloys and Compounds

journal homepage: www.elsevier.com/locate/jalcom

Deformation behavior of $Mg_{67}Zn_{28}Ca_5$ metallic glass at near supercooled liquid region

X.L. Fu [a,*], M.J. Tan [a,*], Y.S. Wang [a], A.E.W. Jarfors [b,c], M. Gupta [d]

[a] Sch. of Mech. and Aerospace Eng., Nanyang Technological University, Singapore 639798, Singapore
[b] Singapore Institute of Manufacturing Technology, Singapore 638075, Singapore
[c] School of Engineering, Jönköping University, Jönköping 551 11, Sweden
[d] Dept. of Mechanical Engineering, National University of Singapore, Singapore 117576, Singapore

ARTICLE INFO

Article history:
Received 30 April 2012
Received in revised form 8 September 2012
Accepted 10 September 2012
Available online 27 September 2012

Keywords:
Amorphous alloys
Strain rate sensitivity
High-temperature deformation
Compression test

ABSTRACT

A systematic study of $Mg_{67}Zn_{28}Ca_5$ amorphous alloy was made at near supercooled liquid region with strain rates ranging from 10^{-6} to 10^{-3} s^{-1}. Compressive deformation behavior showed a transition from inhomogeneous to homogeneous flow. The strain rate sensitivity below the glass transition temperature was approximately 0.27, while in the supercooled liquid region, strain rate sensitivity approached a value of 1. Crystallinity and phase presence in material, were examined by XRD, DSC and TEM. before and after deformation.

1. Introduction

The first Mg-based amorphous alloy was reported in 1977 [1] by Calka et al. Since then, properties of Mg-based amorphous alloys have been investigated extensively. Compared to crystalline magnesium alloys, Mg-based amorphous alloys exhibit a significantly higher yield strength [2], better wear resistance owing to the absence of crystalline lattice and the associated dislocation defects. Lately, it has been found that MgZnCa amorphous alloy displayed tissue compatibility in both in vitro and in vivo degradation tests without clinically observable hydrogen production [3]. One of the advantages of amorphous alloys is the net-shape forming ability, which means metallic glasses like plastics, can be molded into complicate shape parts at near supercooled liquid region [4].

Plastic deformation of a monolithic metallic glass occurs by two major modes: inhomogeneous deformation and homogeneous deformation [5–9]. At high stress and low temperature, plastic deformation is inhomogeneous: the strain is concentrated in a few thin shear bands [10]. The fracture morphology normally exhibits a characteristic "vein" or "river" pattern. At lower stresses and higher temperature, the deformation is homogeneous: every volume of the material undergoes the same strain. Homogeneous deformation can be divided into two different types of flows: non-Newtonian and Newtonian flow. At lower strain rates, bulk metallic glasses behave like a Newtonian fluid but plastic flow becomes non-Newtonian at higher strain rates. Homogeneous deformation was previously predicted to take place at about 0.7 T_g [9]. At below the glass transition temperature, the strain rate sensitivity value m is usually smaller than 0.25. Within supercooled liquid region, the homogeneous deformation can transit from non-Newtonian into Newtonian behavior, the strain rate sensitivity approaches 1.

As a potential biocompatible material, $Mg_{67}Zn_{28}Ca_5$ exhibits quite narrow supercooled liquid region as shown in Refs. [11,12]. In this paper, the deformation behavior at below and above glass transition temperature has been studied over various strain rates and temperatures. A clear transition from inhomogeneous to homogeneous deformation has been shown. The homogeneous deformation can be divided into non-Newtonian and Newtonian flow.

2. Experimental procedure

The $Mg_{67}Zn_{28}Ca_5$ bulk metallic glass was prepared in stages using high purity Mg (99.9 wt.%), Zn (99.99 wt.%) and $Mg_{70}Ca_{30}$ (99 wt.%). As a first step. The pre-melt $Mg_{67}Zn_{28}Ca_5$ alloy was prepared using the technique of disintegrated melt deposition (DMD) [13]. All of the raw materials were heated up to 850 °C in an inert Ar gas atmosphere in a graphite crucible using a resistance heating furnace. The crucible was equipped with an arrangement for bottom pouring. Upon reaching the superheat temperature, the molten slurry was stirred for 5 min at 450 rev min^{-1} to make the alloys homogeneously mix without oxidation. The melt was then released through a 10 mm diameter orifice at the base of the crucible. The melt was

* Corresponding authors.
E-mail addresses: xlfu@ntu.edu.sg (X.L. Fu), mmjtan@ntu.edu.sg (M.J. Tan), yswang@ntu.edu.sg (Y.S. Wang), andersj@SIMTech.a-star.edu.sg (A.E.W. Jarfors), mpegm@nus.edu.sg (M. Gupta).

0925-8388/$ - see front matter
http://dx.doi.org/10.1016/j.jallcom.2012.09.044

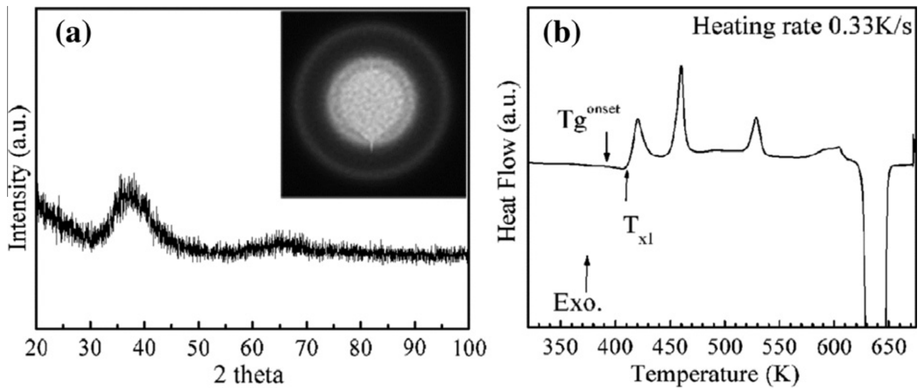

Fig. 1. The microstructural observations on the as-cast metallic glass (a) XRD inset: TEM SEAD pattern and (b) DSC scan of $Mg_{67}Zn_{28}Ca_5$ amorphous sample at a heating rate of 20 K/min.

disintegrated by two jets of argon gas orientated normal to the melt stream. The argon gas flow rate was maintained at 25 L min^{-1}. The disintegrated melt slurry was subsequently deposited onto a metallic substrate. $Mg_{67}Zn_{28}Ca_5$ master alloy with 40 mm diameter was obtained following the deposition stage [14]. In the final stage, about 4.5 g of master alloy were cut from the master alloy and then remelted in a Boron Nitride crucible under vacuum 0.8 atm. The alloy were then heated up by an induction heater with about 7.5 min and finally injected into a copper mold under pressure 1.8 Bar. The rods were made with 2 mm in diameter and 35 mm in length.

Only the bottom 20 mm of the rods were used for mechanical testing. The as-cast rods were carefully examined under XRD using PANalytical Empyrean. The XRD pattern of as-cast metallic glass is shown in Fig. 1(a). The selected specimens show a broad diffused peak without any detectable crystallized peaks. Fig. 1(a) inset shows TEM (using JEOL, JEM-2010) on selected area electron diffraction SAED. A diffuse amorphous ring without any crystalline features further confirmed that the as-cast samples used for compression testing had only amorphous structure and contained no crystalline phases.

The values of the onset of glass transition and crystallization temperature were determined by differential scanning calorimeter (TA instruments DSC Q200) at a heating rate of 20 K/min. Fig. 1(b) shows the glass transition temperature (T_g) and first crystallization temperature (T_{x1}) are 383 K and 411 K, respectively. The supercooled liquid region, which is defined as the difference between crystallization temperature and glass transition temperature, is about 28 K. The supercooled liquid region is very narrow compared to other studied materials with compositions such as $Zr_{41.2}Ti_{13.8}Cu_{12.5}Ni_{10}Be_{22.5}$ [15], $Pd_{40}Ni_{40}P_{20}$ [16], $Zr_{49}Cu_{45}Al_6$ [7], $La_{62}Al_{14}Cu_{12}Ni_{12}$ [8] which usually is above 40 K.

The as-cast samples were then cut into 1.9 mm in diameter and 4 mm in height and prepared for compression testing. Considering the difficulty to machine the brittle material into dog-shaped tensile specimens and that the subtle imperfections would have a significant effect on compression response [17]; the top and bottom surfaces of compression specimens were polished using a specially designed fixture to ensure the flatness and parallelity. The high temperature compression tests were conducted on a Shimadzu Airservo 4830 machine, using a three-zone clamshell furnace with temperature control to within ±1 K. The displacement rate of the crosshead was held constant for any given test, and was varied to give engineering strain rates from the range 1×10^{-3} to $2.5 \times 10^{-6}\ s^{-1}$. The tested temperature range is from 368 K to 408 K. The furnace was preheated to the requested temperature before loading the sample. Generally 20 min was required to equilibrate the system, after which the test was initiated. After each compression test, the sample was immediately taken out and air-cooled to prevent further crystallization.

3. Results and discussion

3.1. Strain rate effect and temperature effect

Fig. 2(a) presents the true stress–strain curve at a constant T = 393 K as strain rates decreases from 10^{-3} to $2.5 \times 10^{-6}\ s^{-1}$. At a relatively higher strain rate $10^{-3}\ s^{-1}$, the compression behavior shows a typical inhomogeneous deformation behavior with no obvious plasticity observed. The failure strength is about 629 MPa, which is in line with other reported MgZnCa amorphous alloy [12]. The fracture surface is carefully observed under high resolution SEM as shown inset (i). Similar to that observed in $Mg_{65}Cu_{25}Tb_{10}$ metallic glass [18], the metallic glass shows a 100–200 nm scale plastic process zone in this very brittle glass. It is reasonable that this "intrinsically brittle" material displays a very fine vein pattern compared to Ti-based metallic glass [18] which have higher toughness.

In Fig. 2(a), at an intermediate test strain rates 2×10^{-4}–$2.5 \times 10^{-5}\ s^{-1}$, the deformation changes from inhomogeneous to homogeneous plastic flow. Inset (ii) is an example shows specimen can be deformed to about 140% at T = 393 K with strain rate $2 \times 10^{-4}\ s^{-1}$; the deformed specimen shows shiny metallic surface and no brittle cracks appeared on the deformed sample. During the tested window, the specimen either deformed by shear localization or exhibit superplasticity. There is no gradual transition has been observed. This homogeneous flow has been explained as a competition between two processes: a shear-induced disordering and a diffusion controlled reordering process [5]. Before the process reaches a steady-state flow condition, there is a structural transience: the stress–strain curve exhibits a peak and a decrease in stress with further applied strain. As the structural relaxation gradually catches up the production of free volume, the steady-state flow is eventually achieved. The overshoot stress is thus defined as the difference between the peak and the steady-state flow stress. This behavior has also been found in other Zr-based [7] and La-based [8] metallic glass.

Fig. 2(b) displays the strain rate effect at different temperatures when the strain rate is at a constant initial strain rate $2.5 \times 10^{-6}\ s^{-1}$. The testing time is usually longer than 679 min. At T = 368 K and 378 K, the steady-state flow stresses fluctuate at a very small degree, which was possibly affected by the machine noise over more than 10 h of continuous testing, indicating the specimen did not undergo significant structural evolution or nanocrystallization at below glass transition temperature even with a very long time of annealing and stress. When T = 393 K and 408 K (the temperature increases to above the glass transition temperature), the stress goes up afar reaching a plateau.

3.2. Deformation mechanism of $Mg_{67}Zn_{28}Ca_5$ amorphous alloy

To understand the steady-state flow stress at various strain rates for different temperatures, especially for temperatures below and above T_g. The relationship between the steady-state flow stress and strain rates has been shown in Fig. 3. On the double-logarithmic plot of Fig. 3; for lower testing temperature T = 368 and 378 K, T = 368 K shows slightly higher flow stress than T = 378 K. Both of them showed that as strain rates changes from 10^{-3} to $2.5 \times 10^{-6}\ s^{-1}$, the strain rate sensitivity, defined as $m = \partial(\log\sigma)/\partial(\log\dot{\varepsilon})$, is approximately 0.27. This result is quite similar as previous findings as in $Zr_{65}Al_{10}Ni_{10}Cu_{15}$ [19] and $Pd_{40}Ni_{40}P_{20}$ [16]. As temperature continue increasing to above the glass transition temperature range (T = 393 and 408 K), the strain rate sensitivity, approaches the Newtonian limit where $m \approx 1$.